March 2008

Simulation of refrigeration by electron emission across nanometer-scale gaps

Tyler Westover
Purdue University - Main Campus, twestove@purdue.edu

Timothy Fisher
Birck Nanotechnology Center, Purdue University, tsfisher@purdue.edu

Simulation of refrigeration by electron emission across nanometer-scale gaps

Tyler L. Westover and Timothy S. Fisher*
School of Mechanical Engineering and Birck Nanotechnology Center, Purdue University, West Lafayette, Indiana 47907, USA
(Received 7 November 2007; revised manuscript received 11 February 2008; published 17 March 2008)

Nanoscale transport processes offer new possibilities for direct refrigeration by electron emission at room temperature. Because the energy of emitted electrons may be higher or lower than that of their replacement counterparts, a heating or cooling effect, known as the Nottingham effect, can occur at the emitter. Prior theoretical studies indicate the possibility of very large (>100 W/cm^2) cooling rates for emitters with low work functions; however, ultrasmall emission gaps are necessary to produce a device with a reasonably high coefficient of performance. In this regime of low work function and narrow emission gap, the traditional approach used to model electron transmission, which is based on the WKB approximation, is not suitable. In this study, a nonequilibrium Green's function method is employed to simulate the energy exchange attending electron emission for a range of emitter work functions and vacuum gap distances, yielding important insights into the thermodynamics associated with electron emission across ultrasmall vacuum gaps. Cooling density and efficiency curves depending on the vacuum gap distance and applied electric field are presented for flat-plate electrodes with work functions ranging from 0.4 to 1.7 eV, and the results indicate that a practical emission device will require that the electrode work function and vacuum gap separation be reduced to approximately 0.4 eV and 20 nm, respectively.

DOI: 10.1103/PhysRevB.77.115426 PACS number(s): 72.15.Jf, 79.40.+z, 79.70.+q, 73.23.−b

I. INTRODUCTION

Refrigeration by thermionic electron emission across a vacuum gap has been considered for many years, although, as Mahan suggested in 1994,[1] such devices are limited to high temperatures because of the lack of suitable emitter materials with work functions below approximately 0.3 eV. However, continuing advances in microscale and nanoscale devices offer new possibilities for achieving low-temperature refrigeration by the emission of electrons across nanoscale vacuum gaps. High-energy electrons can escape from a surface by emitting over the surface potential barrier (thermionic emission), while low-energy electrons can penetrate through thin potential energy barriers by quantum tunneling (field emission).[2] The local energy exchange that results from electron emission, known as the Nottingham effect, may produce heating or cooling depending on the average energy of the emitted electrons relative to that of the electrons that replace them. Refrigeration occurs when the emission of high-energy electrons is favored through filtering processes that depend on geometric scale effects,[3] Schottky depletion,[4] and resonant-tunneling phenomena.[5] For example, Hishinuma *et al.* showed that reducing the vacuum gap between the emitter and collector significantly reduces the emission barrier and reported room-temperature cooling of a few millikelvin.[6] The use of nanostructured field emitters, such as carbon nanotubes, may also significantly increase the refrigeration achievable at room temperature.[7] The local electric field at small tips greatly increases the cooling power by amplifying the field emission current[8] and by favoring the emission of high-energy electrons.[9] Quantum confinement in nanoscale emitter structures may also enhance cooling performance by restricting electron momentum perpendicular to the direction of transport.[10]

Realization of refrigeration by electron emission at room temperature will depend on a thorough understanding of how nanoscale features affect energy transport and the ability to fabricate devices capable of exploiting these possibilities. Unfortunately, the quantum phenomena inherent in such devices are not well captured by traditional models that rely on Richardson's equation for thermionic emission and the Wentzel–Kramers–Brillouin (WKB) approximation for field emission. Further, these models do not apply to electron emission from low-work function emitters separated by a nanometer vacuum gap—the most promising conditions for a vacuum-gap emission refrigerator. The present work employs a nonequilibrium Green's function (NEGF) approach to accurately simulate the quantum transmission of electrons across a vacuum gap and provides important insights into the factors that affect total cooling power and efficiency of a one-dimensional device operating under ideal conditions.

Numerous experimental studies have investigated the energy exchange attending electron emission. Swanson *et al.*[11] conducted extensive experiments measuring the heat exchange involved in emission from high and low work function wires in the temperature range 300–1160 K and demonstrated the transition of the Nottingham effect from heating to cooling. Bergeret *et al.*[12] measured Nottingham heating in the absence of Joule heating using niobium superconducting samples. Xu *et al.*[13] investigated the heat transfer between a scanning tunneling microscope (STM) tip and a sample surface by integrating planar thermocouples into the STM tips and reported Nottingham heating with a sensitivity of 10 nW. Recently, Hishinuma *et al.*[14] reported an estimated cooling effect of 1–10 nW produced by thermionic emission across a nanometer gap at room temperature.

The present work employs the NEGF method to predict the effects of emitter work function and vacuum gap distance on this electrical-thermal energy conversion process. Efficient cooling requires that the majority of electrons emitting across the gap originate from energy states above the emitter's Fermi level and that these electrons tunnel through the vacuum barrier near the barrier peak. Unfortunately, the

WKB approximation is not applicable in this regime.[15] In addition, because the WKB approximation involves an integral along the electron's trajectory through the potential barrier, it is not well suited to calculate electron transmission probabilities across complicated potential barriers, such as those incorporating image charges from multiple electrodes and/or space charge.

Under these conditions, numerical methods, such as transfer matrix,[16] Airy function,[17] and NEGF[18] approaches, must be employed to model quantum tunneling. These methods numerically solve Schrödinger's equation in the barrier region and are valid for electrons of all incident energies. Additional advantages embodied in these numerical methods include the ability to account for space-charge and band-structure effects, as well as quantum confinement and other effects relating to the wavelike nature of electrons. The NEGF simulation approach is chosen in this work because it is efficient and straightforward for nanometer-size device modeling.[19] An Airy function approach is also employed for some cases to validate the NEGF results, although accurately determining the values of the Airy functions and their derivatives over a wide range of values necessary to solve field emission problems is computationally expensive.

We note that although prior work has employed exact quantum simulations to determine the error introduced by the WKB approximation in estimating the total emission current from a low work function planar electrode,[20] a similar study exploring the limitations of the WKB approximation for calculating the energy exchange at the emitter surface has not yet appeared in the literature. In this work, we show that using the WKB approximation introduces substantial error in predicting room-temperature cooling by electron emission because the electron transport in this situation is dominated by electrons with energies near the peak of the vacuum potential energy barrier—the regime in which the WKB approximation is not applicable.

In subsequent sections, the electron emission model is first outlined, and the equations to be solved are presented. Then, the basic principles underlying the NEGF simulation are summarized, after which results obtained using the NEGF method are compared to those obtained from the WKB approximation and Airy function approaches for flat-plate field emission from emitters with work functions of 0.7, 1.7, and 3.5 eV. This example establishes the accuracy of the NEGF and Airy function approaches and illustrates the limitations of the WKB approximation for an accurate modeling of energy exchange, particularly for low work function emitters. In the last section, the NEGF simulation is applied to flat-plate electrodes emitting across a nanometer vacuum gap, and results are presented to illustrate the influence of the electrode work functions, vacuum gap distance, applied electric field, and space charge in the vacuum region.

II. ELECTRON EMISSION

A. Emission current

The theory of electron emission has been described in detail by Good and Müller.[21] Consequently, only a brief summary of the major results is provided here. The application of an electric field between two closely spaced electrodes produces a potential energy field of the form[22]

$$U(x) = \frac{\phi}{q} - Fx - \frac{q}{4\pi\varepsilon_0}\left(\frac{1}{4x}\right) + U_{\text{anode}}(x) + U_{scf}(x), \quad (1)$$

where q is the magnitude of the electron charge, x is the distance from the emitter, F is the applied electric field, and ε_0 is the permittivity of free space. The last term in Eq. (1) represents the self-consistent increase in the potential energy profile due to space-charge effects and is negligible for nearly all practical cooling applications, as shown in the Appendix. The third term on the right side is the classical correction due to image charge effects from the emitter (cathode), and $U_{anode}(x)$ is the image potential due to the collector (anode). Equation (1) assumes that the emitter and collector have similar work functions, and in this case $U_{anode}(x)$ can be estimated using semiclassical theory as[22]

$$U_{anode}(x) = -\frac{q}{8\pi\varepsilon_0}\sum_{n=1}^{\infty}\left(\frac{nd}{n^2d^2 - x^2} - \frac{1}{nd}\right), \quad (2)$$

where the infinite series represents the effects of reflections of the image charge on the electrode surfaces. In reality, the image charge potential between two closely spaced electrodes is a quantum mechanical phenomenon involving infinite numbers of charges in both electrodes,[23] making exact solutions elusive. For this reason, a semiclassical approximation is chosen to estimate the potential barrier reduction due to image charges from both electrodes. More importantly, however, electron emission across a nanometer vacuum gap is quite sensitive to the exact form of the image charge potential reduction; consequently, experimental validation of Eq. (2) is needed in order to ensure an accurate simulation of electron emission across a nanometer vacuum gap.

The potential profile in Eq. (1) differs in three respects with the development by Good and Müller.[21] In the present work, the zero energy datum is located at the emitter's Fermi energy, instead of at the vacuum level; also, Good and Müller neglected the image charge correction due to the anode $U_{anode}(x)$ and the self-consistent increase in the potential energy profile due to space-charge effects $U_{scf}(x)$.

The total emission current density J from the emitter due to the electric field is given by

$$J = q\int_{-W_a}^{\infty} N(W)D(W)dW, \quad (3)$$

where $-W_a$ represents the bottom of the emitter's conduction band, W is the electron energy associated with the x component of momentum, $N(W)$ is the electron supply function, and $D(W)$ is the quantum tunneling transmission function. Traditionally, the transmission function has been calculated using the WKB approximation,[24]

$$D(W) = s(W)\exp\left\{\int_{x_1}^{x_2}\frac{1}{\hbar}\sqrt{8m|U(x) - W|}dx\right\}, \quad (4)$$

where $s(W)$ is a slowly varying function of W that depends on the shape of the energy potential barrier $U(x)$ and is often

approximated as unity. x_1 and x_2 are the zeros of $U(x)-W$, and m is the rest mass of an electron. In general, the WKB approximation is limited to relatively low fields and high work functions, and is not applicable to electrons with energies near the barrier peak. For electrons that have sufficient energy to pass over the barrier, the transmission function is taken as unity. The supply function $N(W)$ in Eq. (3) represents the number of electrons incident on the emitter surface per second per unit area and can expressed analytically as[21]

$$N(W)dW = \frac{4\pi m k_B T}{h^3} \ln\left\{1 + \exp\left[-\frac{W}{k_B T}\right]\right\} dW, \quad (5)$$

where h is Planck's constant, k_B is Boltzmann's constant, and T is the emitter temperature.

B. Energy transport

The rate of net energy flux from the emitter due to electron emission may be found by multiplying the total emission current density [Eq. (3)] by the total average energy difference between the emitted and replacement electrons and dividing by the electronic charge per electron,

$$Q'' = \frac{J}{q}(\langle \varepsilon_{emit} \rangle - \langle \varepsilon_{repl} \rangle) = \frac{J}{q}\Delta\varepsilon, \quad (6)$$

where $\langle \varepsilon_{emit} \rangle$ and $\langle \varepsilon_{repl} \rangle$ are the average total energies of the emitted and replacement electrons, respectively. Chung *et al.*[25] were the first to calculate the average energy of the replacement electrons and found that $\langle \varepsilon_{repl} \rangle$ could lie as much as 50 meV below the Fermi level. Here, we follow the work of Fisher and Walker[26] who separated the emitted and replacement energies into axial and transverse components (in the emission direction and perpendicular to the emission direction, respectively). Thus, Q'' becomes

$$Q'' = \frac{J}{q}(\langle W_{emit} \rangle + \langle \Gamma_{emit} \rangle - \langle W_{repl} \rangle - \langle \Gamma_{repl} \rangle), \quad (7)$$

where Γ represents energy associated with momentum in the transverse direction, and the subscripts *emit* and *repl* refer to emitted and replacement electrons, respectively. This separation is possible because the energy associated with electron motion perpendicular to the surface normal does not interact with the potential field in the vacuum region. Thus, in order to determine the heating or cooling per unit area at the emitter, it is necessary to calculate the average normal and transverse energies of the emitted and replacement electrons.

The average energy of the emitted electrons in the longitudinal direction $\langle W_{emit} \rangle$ is calculated by taking an energy moment of Eq. (3) and dividing by the total current density. The average energies of the replacement electrons can be computed by recognizing that the emitted electrons leave vacant states near the surface of the emitter. Expressions for $\langle \Gamma_{emit} \rangle$, $\langle W_{repl} \rangle$, and $\langle \Gamma_{repl} \rangle$ as functions of $D(W)$ and $f(\mathrm{W}, \rho)$ have been previously given by Fisher and Walker[26] and are not repeated here. The present work differs from that of Fisher and Walker[26] in two respects; first, the transmission function $D(W)$ has been calculated using the nonequilibrium Green's function method instead of the less accurate WKB approximation. Second, the present work includes the image potential terms from the anode [Eq. (2)], which is significant for vacuum gap distances approaching a few nanometers.

C. Efficiency

For electron emission devices, performance is often assessed in terms of a so-called electronic efficiency, which is the efficiency associated solely with electronic transport under ideal conditions, neglecting all parasitic losses.[27] Overall device efficiency is always less than the electronic efficiency but may approach the electronic efficiency as an upper limit. In the case of a refrigeration device, electronic efficiency may be represented as a coefficient of performance (COP), which is defined as the ratio of the output cooling power to the required electrical consumption. Assuming ideal conditions and neglecting all parasitic losses, the (COP) can be expressed as

$$\mathrm{COP} = \frac{J\Delta\varepsilon}{JV_{bias}} = \frac{\Delta\varepsilon}{Fd}, \quad (8)$$

where d is the vacuum gap distance separating the electrodes.

III. NONEQUILIBIUM GREEN'S FUNCTION FORMALISM

The NEGF approach is an established and powerful tool for studying quantum transport and has been described in detail by Datta.[18] This section briefly outlines the NEGF algorithm used to calculate the quantum transmission function $D(W)$ in Eq. (3). We start with the time-independent, one-dimensional Schrödinger equation[24]

$$-\frac{\hbar^2}{2m}\frac{d^2\Psi}{dx^2} + U\Psi = E\Psi \Rightarrow H\Psi = E\Psi, \quad (9)$$

where H is the Hamiltonian operator, which may be formulated as a tridiagonal matrix by discretizing the calculation domain and then employing finite differences to approximate the second order derivative of the wave function with respect to position.[18] The first grid point is located on the emitter (cathode) surface, and the last is located on the collector (anode) surface, while the rest of the grid points are distributed over the vacuum region with uniform grid spacing a. In the Green's function formalism, the transmission function $D(W)$ is given by[18]

$$D(W) = \mathrm{trace}[\Gamma_1 G^R \Gamma_2 (G^R)^\dagger], \quad (10)$$

where G^R is the retarded Green's function matrix and the '†' superscript indicates the complex conjugate transpose operation. Γ_1 and Γ_2 are energy broadening matrices that are defined below. The retarded Green's function can be expressed as

$$G^R(W) = [(W + i0^+)I - H - \Sigma_1(W) - \Sigma_2(W)]^{-1}, \quad (11)$$

where Σ_i are the self-energy matrices and $i0^+$ is a small imaginary perturbation introduced to make the system irreversible. All effects due to excitations from the emitter and

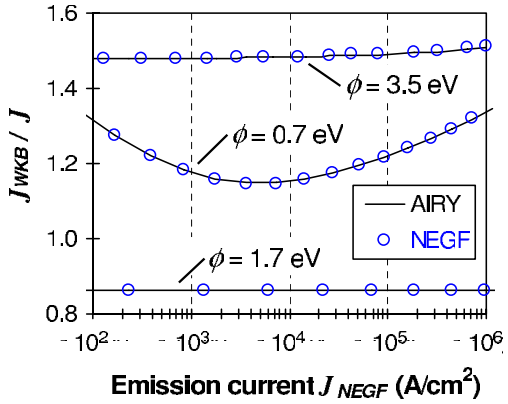

FIG. 1. (Color online) Ratios of the total emission current calculated using the WKB approximation to that calculated using the NEGF and Airy function approaches for flat-plate emitters with ϕ =0.7, 1.7, and 3.5 eV. T=300 K and d>15 nm.

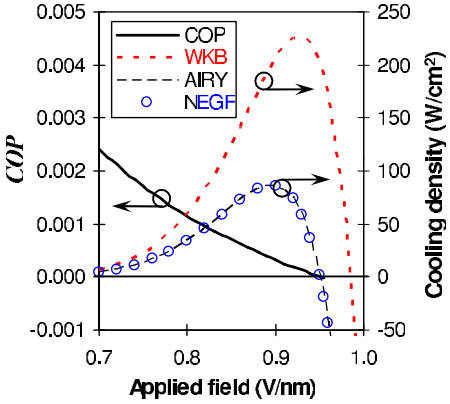

FIG. 2. (Color online) Predicted net energy exchange at emitter (cathode) for a flat-plate emitter using the WKB, Airy function, and NEGF approaches. The coefficient of performance was estimated using the NEGF approach. ϕ=1.7 eV, T=300 K, and d=20 nm.

collector are accounted for in the self-energy matrices of Eq. (11). Assuming that the emitter is semi-infinite, $\Sigma_1(W)$ can be simplified such that all terms are zero except for the first term $\Sigma_1(1,1)$, which is given by $-t_0 \exp(ik_1a)$, where $t_0 = \hbar^2/(2ma^2)$ and k_1a is defined by $W = U_1 + 2t_0(1-\cos k_1a)$. Similarly, $\Sigma_2(W)$ can be simplified such that the only nonzero term is the last term $\Sigma_2(N,N)$, which is given by $-t_0 \exp(ik_Na)$, where k_Na is defined by $W = U_N + 2t_0(1 - \cos k_Na)$.

To finish the calculation for the transmission function, we define the broadening matrices Γ_1 and Γ_2, which describe the electron exchange rate between the vacuum and the contacts. They may be written in terms of the self-energy matrices as

$$\Gamma_j = i[\Sigma_j - \Sigma_j^\dagger]. \tag{12}$$

We note that because the broadening matrices Γ_1 and Γ_2 each have only a single nonzero term, evaluating the quantum transmission function in Eq. (10) only requires the final column of G^R, which can be calculated efficiently because H is tridiagonal. The quantum transmission function can also be computed efficiently using the contact block reduction method outlined by Mamaluy *et al.*[19] In this approach, the eigenvectors of a decoupled device Hamiltonian matrix need be determined only once. Thereafter, the transmission function $D(W)$ is calculated using 2×2 matrices, which represent the portion of the retarded Green's function that corresponds to the contacts.

IV. RESULTS

A. Comparison of the WKB, NEGF, and Airy function approaches

1. Total emission current

Figure 1 shows the ratios of the total emission current calculated using the WKB approximation to that calculated using the NEGF and Airy function approaches for flat-plate emitters with ϕ=0.7, 1.7, and 3.5 eV. The integral in Eq. (3) was evaluated numerically using the WKB, NEGF, and Airy function approaches independently to calculate the transmission function for each value of W. Also in Fig. 1, the vacuum gap distance d is assumed to be greater than approximately 15 nm so that the image charge correction due to the anode [Eq. (2)] can be neglected. For the emission currents represented in Fig. 1, space charge is negligible, as shown in the Appendix; therefore, $U_{scf}(x)$ in Eq. (2) has also been neglected. For the curves shown, the total emission current predicted by the NEGF and Airy function approaches differs by less than 0.25%, illustrating the accuracy of both. The error associated with the WKB approximation is considerably larger, although still less than 50% for all curves. For relatively large values of ϕ, the ratio of the total emission current calculated by the WKB approximation to the exact emission current is nearly independent of the emission current, indicating that the error is principally caused by approximating the function $s(W)$ in Eq. (4) as unity. For ϕ =0.7 eV, the ratio of the total emission current calculated by the WKB approximation to the exact emission current is not constant because the WKB approximation is not applicable to low work function emitters as explained earlier because a significant portion of the emitted electrons possess energies near the potential barrier peak, as will be shown in the next section.

2. Energy exchange at the emitter surface

The error that arises in using the WKB approximation to model the energy exchange process as outlined in Eqs. (3)–(7) is even more pronounced. Figure 2 shows the calculated cooling density due to the Nottingham effect as a function of applied field for a flat emitter with ϕ=1.7 eV using the WKB, NEGF, and Airy function approaches. As the applied field increases, the emission current rises exponentially, increasing the cooling effect at the emitter. However, as the applied field increases, the net energy exchange per electron decreases and ultimately becomes negative, producing heating at the emitter surface. The maximum error between the energy exchange curves calculated by the NEGF and Airy function approaches in Fig. 2 is less than 0.3%. In contrast, the WKB approximation overpredicts the maximum cooling effect at the surface by a factor of approximately 3 and also

significantly overpredicts the critical electric field at which the Nottingham effect transitions from cooling to heating. The error trends in Fig. 2 are similar for other values of the emitter work function, although as ϕ increases above 1.7 eV, the maximum predicted cooling at room temperature quickly approaches zero. The predicted electronic COP calculated using the NEGF approach is also included in Fig. 2 and reveals that refrigeration from such a device would be extremely inefficient. The necessary conditions to increase the COP are discussed below.

B. Optimal conditions for a cooling device

1. Overview

This section focuses on the optimization of a field emission refrigeration device and provides sample calculations illustrating the effects of the relevant parameters on such a device. The ideal potential barrier to maximize the cooling efficiency of a flat-plate field emission device is a moderately thick, nearly rectangular barrier. For such a barrier, the quantum tunneling transmission function decreases very rapidly as the electron energy falls below the top of the barrier; yet, the transmission function is nearly unity for electrons with energies greater than the barrier height. Thus, only high-energy electrons are emitted, and the cooling efficiency is maximized as long as the top of the barrier lies above the emitter's Fermi energy.

Figure 3(a) shows the potential energy field in the vacuum region near an emitter with ϕ=0.7 eV subject to applied electric fields of 0.1 and 0.4 V/nm. The bare solid lines correspond to the potential barrier formed between parallel electrodes separated by a large vacuum gap for which $U_{anode}(x)$ is negligible, and the solid lines with triangles correspond to electrodes separated by a vacuum gap of 6 nm for which $U_{anode}(x)$ in Eq. (1) is significant. As the applied electric field increases from 0.1 to 0.4 V/nm, the barrier peak becomes more pronounced and decreases below the Fermi energy. The resulting effects enhance the emission of lower energy electrons and consequently shift the electron energy distributions to lower energies. Figure 3(b) shows the normalized longitudinal energy distributions of electrons emitted across the four potential energy barriers of Fig. 3(a) and illustrates the strong effect of the applied electric field on the emitted electron energy distributions as well as the weaker effect of the vacuum gap distance.

A high cooling density requires that the emission current J and the net energy exchange per electron $\Delta\varepsilon$ should be large. From Eq. (8), maintaining a high COP in a field-emission refrigeration device also requires maximizing $\Delta\varepsilon$; however, the electric field and the vacuum gap distance must be minimized. Figure 3(a) shows that these conditions produce opposing effects. Increasing the applied electric field reduces the potential barrier and causes an exponential increase in emission current [see Eq. (4)]; yet, increasing the electric field also decreases the average energy of emitted electrons and thus reduces $\Delta\varepsilon$. Consequently, increasing the electric field reduces the COP of a field emission refrigeration device both by decreasing $\Delta\varepsilon$ and by increasing the power density supplied to the device, JFd. Figure 3(b) reveals further that

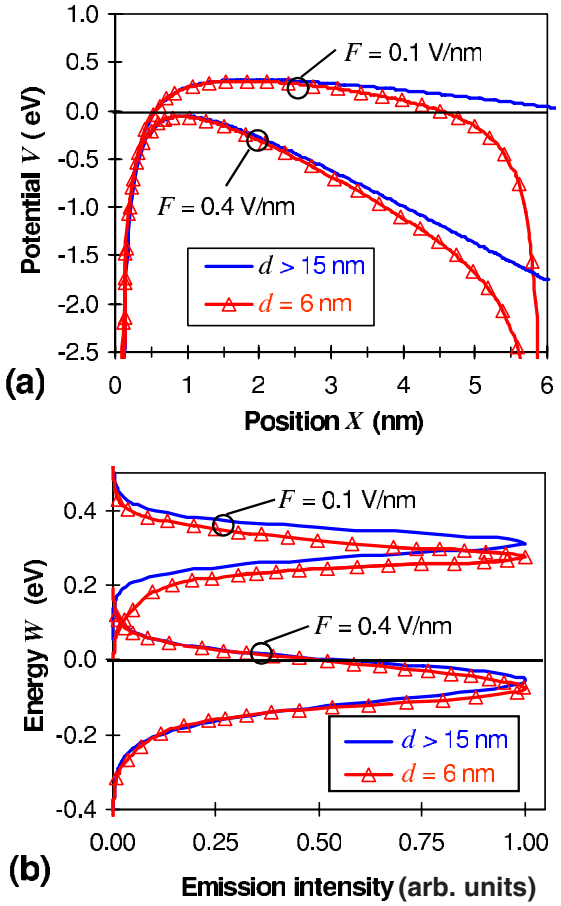

FIG. 3. (Color online) (a) Potential energy field of a 0.7 eV emitter subject to applied electric fields of 0.1 and 0.4 V/nm. Potential barriers are shown for $d>15$ nm (solid lines) and for $d=6$ nm (solid lines with triangles). T=300 K. (b) Normalized energy distributions of electrons emitted across the potential energy barriers in (a).

decreasing the electrode separation distance to 6 nm also slightly reduces $\Delta\varepsilon$, and this effect is examined in the next section.

2. Effects of emitter work function and vacuum gap distance

From the above discussion, it is apparent that the applied electric field must be as low as possible for an optimal cooling device; therefore, the electrode work functions must be as small as possible to reduce the potential energy barrier encountered by emitting electrons. Surfaces with work functions as low as 0.7 eV have been reported by evaporating cesium on tungsten or silver to form $W_2$0-Cs (Ref. 28) or $Ag_2$0-Cs (Ref. 29), respectively. Work functions below 0.7 eV have been reported from unstable compounds involving alkalides and electrides; however, stable emitters of these compounds have not been demonstrated.[30] In addition to obtaining a low work function emitter, the vacuum gap distance between the electrodes should be optimized to improve the electronic coefficient of performance. Assuming that a nanometer-scale vacuum gap distance can be achieved and maintained over a sufficiently large area to be useful, the electrode separation distance should be reduced until the net

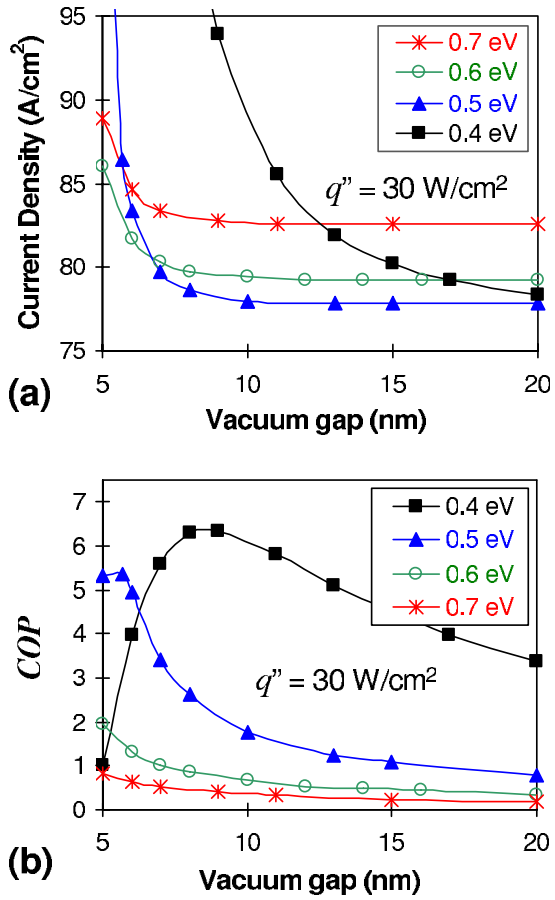

FIG. 4. (Color online) (a) Predicted net current density and (b) electronic coefficient of performance as functions of electrode separation distance for a flat-plate field emitter with ϕ ranging from 0.4 to 0.6 eV. All curves correspond to a cooling density of 30 W/cm^2 with emitter and collector temperatures of 300 and 340 K, respectively.

energy exchange per electron begins decreasing rapidly, so that a larger emission current would be necessary to maintain the desired cooling density.

Figure 4 contains predicted coefficient of performance and current density graphs as functions of the vacuum gap separation distance for work functions ranging from 0.4 to 0.7 eV. All curves correspond to a condition in which the emission current is adjusted as needed such that a fixed emitter cooling density of 30 W/cm^2 is achieved. For the curves in Fig. 4, reverse electron emission from the collector to the emitter is significant, and this effect has been taken into account by assuming that the emitter and collector temperatures are 300 and 340 K, respectively. The required current density increases sharply for narrow vacuum gap separation distances because many electrons near the Fermi energy, which do not contribute to cooling, are able to penetrate the vacuum barrier and tunnel to the collector. Figure 4(a) reveals that this effect becomes more pronounced as the electrode work functions decrease. For example, for electrodes with ϕ=0.7 eV, the emission current density required to maintain 30 W/cm^2 of cooling increases rapidly as the vacuum gap decreases below approximately 5 nm. However, for electrodes with ϕ=0.4 eV, the required emission current rises sharply for vacuum gaps below approximately 20 nm. Figure 4(b) shows that the electronic COP increases dramatically as the electrode work function decreases and reaches a maximum of more than 6 for planar electrodes with work functions of 0.4 eV. This COP value approaches that of a Carnot refrigerator (COP=7.5) operating between thermal reservoirs at similar temperatures. Of course, it must be remembered that the high COP values shown in Fig. 4(b) include only the electronic contributions to the total device efficiency and neglect parasitic losses such as heat conduction through electrical contacts and support structures, thermal radiation between the electrodes,[31] and electrical lead losses.

From the above discussion, we see that as the electrode work functions decrease, the ideal vacuum gap distance increases in order to maintain a sufficiently high potential energy barrier to prevent emission of low-energy electrons. For electrode work functions of 0.4 eV operating at a vacuum gap distance of 15 nm, the electronic COP is still nearly 5. If electrode work functions below 0.4 eV can be achieved, even larger electrode separation distances would be feasible; however, as d increases significantly beyond 20 nm, space-charge effects become significant. In reality, however, developing an emitter with a work function of 0.4 eV is unlikely in the near future; consequently, the remainder of this section is devoted to optimize conditions for refrigeration using a 0.7 eV work function emitter. Figure 4 indicates that the optimum vacuum gap for a 0.7 eV work function emitter is approximately 5 nm because the required emission current rises dramatically as the vacuum gap decreases below this value and the coefficient of performance deceases for wider vacuum gaps. Figure 5 shows the predicted cooling density and coefficient of performance for electrodes with ϕ =0.7 eV separated by a vacuum gap of 5 nm. The emitter and collector temperatures are 300 and 340 K, respectively. The lower cooling density curve was calculated self-consistently by the method described in the Appendix, while the higher cooling density curve neglects the self-consistent potential energy component U_{scf}.

As discussed previously, q'' exhibits a maximum and then decreases to zero as the field increases because the net energy exchange per electron $\Delta\varepsilon$ decreases as the electric field increases until it eventually becomes negative, producing heating rather than cooling at the emitter. At high current densities, space-charge effects increase the potential energy barrier and, hence, decrease the total emission current and cooling power. However, as shown in the Appendix, U_{scf} is approximately a quadratic function of position in the vacuum gap region, and this behavior tends to smooth out the sharp peak in the energy barrier and thus increases $\Delta\varepsilon$. The result is that, as shown in Fig. 5, space-charge effects extend the region of cooling to higher applied electric fields.

The COP curve shown in Fig. 5 neglects space-charge effects and decreases with increasing electric field, as discussed previously. The electronic coefficient of performance including space-charge effects is not shown for clarity because it deviates very little from the displayed curve. We also note that the COP shown in Fig. 5 was calculated using Eq. (8) and does not includes parasitic losses, which are expected to be significant, particularly because high current densities

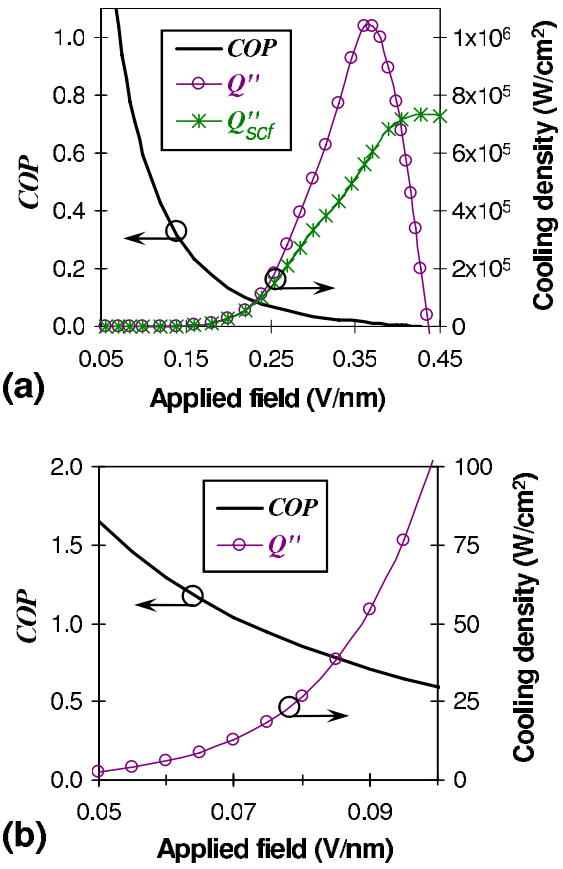

FIG. 5. (Color online) (a) Predicted net energy exchange at the emitter and coefficient of performance for a flat-plate field emitter with $d=5$ nm and $\phi=0.7$ eV. The emitter and collector temperatures are 300 and 340 K, respectively. (b) is a magnification of the low electric field range of (a).

are still needed to obtain the predicted cooling fluxes.[31] For example, the emission current density at maximum cooling is nearly 4×10^8 A/cm^2, corresponding to a net energy exchange per electron of approximately 0.03 eV and a COP less than 2%.

At lower applied electric fields, an electronic COP greater than 1 is possible, although the total cooling density is reduced considerably. As illustrated in Fig. 5(b), the electronic COP is approximately 0.6 for a cooling density of 100 W/cm^2. However, an emission current density of approximately 350 A/cm^2 is still needed to produce this cooling density. Maintaining an emission current of this magnitude would introduce significant parasitic losses not included in the electronic COP calculated here, and thus a work function below 0.7 eV would seem to be necessary to realize a practical refrigeration device operating in a flat-plate configuration.

V. CONCLUSIONS

The WKB, NEGF, and Airy function approaches have been used to simulate electron emission and Nottingham cooling for flat-plate electrodes emitting across a nanometer vacuum gap. The results obtained from the NEGF and Airy function approaches are in excellent agreement and show that the WKB approximation introduces significant error for low work function emitters (<1.7 eV) operating at applied fields of approximately 1 V/nm. The NEGF and Airy function approaches predict that flat-plate electrodes having work functions of 0.7 eV emitting across a narrow gap (3–10 nm) are capable of producing a cooling density of 30 W/cm^2. For such a device, an optimum electrode separation distance exists at approximately 5 nm for which the required emission current is approximately 85 A/cm^2 and the electric coefficient of performance could be as high as 0.84. A similar device with electrode work functions of 0.4 eV operating with a vacuum separation of approximately 15 nm could have an electronic COP as high as 5. In either case, however, parasitic losses and nonideal effects such as undesirable heat conduction through electrical contacts and support structures, Joule heating, and heat transfer between the electrodes through radiation would substantially reduce the device efficiency, and these effects would need to be addressed before a practical field emission refrigeration device could be developed.

ACKNOWLEDGMENTS

The authors wish to thank the National Science Foundation's Nanoscale Science and Engineering program under Award No. CTS-0210366 and the Cooling Technologies Research Center at Purdue University for assistance in funding this project. We are also grateful to Ronald G. Reifenberger of the Purdue Nanophysics Laboratory for many helpful discussions.

APPENDIX

For large electrode separation distances, space-charge effects have been shown to significantly affect field emission for current densities greater than approximately 10^6 A/cm^2 (Ref. 32). For a nanometer-scale vacuum gap distance, several approximations exist to obtain a reasonable estimate of the range of current densities for which space charge significantly affects the energy exchange associated with field emission. First, space-charge effects are considered only for electrons that actually traverse the potential barrier, neglecting electrons that are reflected back to the emitter. Electron-electron scattering is assumed to be negligible, making it possible to model space-charge effects simply using a self-consistent potential that depends only on the electric charge distribution in the vacuum gap region. The first assumption is reasonable because the reflected electrons are only present in a very small region of the vacuum gap where the slope of the potential barrier is very steep. Very high electron densities would be needed to increase the barrier thickness significantly under these conditions. The second approximation is valid for relatively low electron concentrations where the mean free path of the electrons is greater than the vacuum gap separation distance.

Because efficient refrigeration by electron emission is characterized by narrow vacuum gaps and low applied electric fields, it is also assumed that the electron velocity in the

vacuum gap region is constant. This assumption becomes necessary as the vacuum gap distance is reduced to the scale of the electron wavelength because in this situation the local electron velocity is somewhat uncertain.[33] The local charge density actually decreases as the electrons accelerate in the vacuum gap region; hence, this approximation overestimates space-charge effects and places a lower limit on the range of emission currents for which space-charge effects are significant. With these assumptions, the charge density ρ in the vacuum gap region is constant, and Poisson's equation is used to calculate the self-consistent potential,

$$\frac{d^2}{dx^2}U_{scf}(x) = -\frac{\rho}{\varepsilon_0} \tag{A1}$$

The total charge density in the vacuum gap region is determined in the same manner as the total electron emission current—that is, by discretizing the energy distribution and summing the contributions from all discrete energy levels W_i. The charge density ρ_i arising from a discrete energy level is given by J_i/v_i, where J_i is the emission current and v_i is the longitudinal velocity of the electrons with energy W_i. The emission current from each energy level is calculated in the numerical evaluation of Eq. (3), and the longitudinal velocity of electrons with energy W_i is given by

$$v_i = \sqrt{\frac{m}{2q}(W_i + \phi)} \tag{A2}$$

Once J_i, v_i, and ρ_i have been calculated for each discrete energy level, the total charge density in the vacuum gap region is determined by summing all ρ_i. Assuming that ρ is uniform throughout the vacuum region and setting $U_{scf}(x)$ to zero at the electrode surfaces, the solution to Eq. (A1) is

$$U_{scf}(x) = \frac{\rho}{2\varepsilon_0}(xd - x^2). \tag{A3}$$

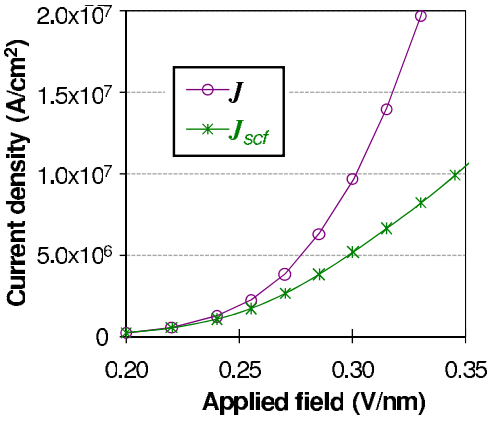

FIG. 6. (Color online) Predicted net current density as a function applied electric field for a flat-plate field emitter with ϕ=0.7 eV. The vacuum gap separation is 5 nm, and the emitter temperature is 300 K.

The procedure to solve for the emission current and potential energy barrier self-consistently entails first solving for the emission current [Eq. (3)], assuming that $U_{scf}(x)$ in Eq. (1) is negligible. Next, $U_{scf}(x)$ is determined based on the calculation for J, and then J is updated using the potential energy field of Eq. (1) including $U_{scf}(x)$. This process is then repeated until convergence is achieved. Figure 6 plots the emission current as a function of applied electric field for flat-plate electrodes (ϕ=0.7 eV) spaced 5 nm apart and compares the self-consistent emission current with the predicted current, assuming that $U_{scf}(x)$ is zero everywhere. In this case, as well as in other cases investigated, space-charge effects become significant when the current density approaches approximately 10^7 A/cm^2, at which point the error is approximately 100% for both the emission current and the cooling density. Thus, space-charge effects are not expected to be significant in any practical cooling device operating with emission currents in the ranges shown in Figs. 4 and 5.

*tsfisher@purdue.edu

[1] G. D. Mahan, J. Appl. Phys. **76**, 4362 (1994).
[2] R. Gomer, *Field Emission and Field Ionization* (Harvard University Press, Cambridge, MA, 1961).
[3] T. S. Fisher and D. G. Walker, ASME J. Heat Transfer **124**, 954 (2002); T. S. Fisher, Appl. Phys. Lett. **79**, 3699 (2001); G. N. Fursey and D. V. Glazanov, J. Vac. Sci. Technol. B **16**, 910 (1998).
[4] N. M. Miskovsky and P. H. Cutler, Appl. Phys. Lett. **75**, 2147 (1999).
[5] A. N. Korotkov and K. K. Likharev, Appl. Phys. Lett. **75**, 2491 (1999); Physica B **284**, 2030 (2000); R. Tsu and R. F. Greene, Electrochem. Solid-State Lett. **2**, 645 (1999).
[6] Y. Hishinuma, T. H. Geballe, B. Y. Moyzhes, and T. W. Kenny, Appl. Phys. Lett. **78**, 2572 (2001); J. Appl. Phys. **94**, 4690 (2003).
[7] N. M. Miskovsky and P. H. Cutler, Appl. Phys. Lett. **75**, 2147 (1999); T. S. Fisher and D. G. Walker, ASME J. Heat Transfer **124**, 954 (2002).
[8] C. A. Spindt, J. Appl. Phys. **39**, 3504 (1968).
[9] N. M. Miskovsky, S. H. Park, J. He, and P. H. Cutler, J. Vac. Sci. Technol. B **11**, 366 (1993); T. S. Fisher, Appl. Phys. Lett. **79**, 3699 (2001).
[10] M. F. O'Dwyer, R. A. Lewis, and C. Zhang, Phys. Rev. B **72**, 205330 (2005).
[11] L. W. Swanson, L. C. Crouser, and F. M. Charbonnier, Phys. Rev. **151**, 327 (1966).
[12] H. Bergeret, A. Septier, and M. Drechsler, Phys. Rev. B **31**, 149 (1985).
[13] J. B. Xu, K. Läuger, R. Möller, K. Drasfeld, and I. H. Wilson, Appl. Phys. A: Solids Surf. **59**, 155 (1994).
[14] Y. Hishinuma, T. H. Geballe, B. Y. Moyzhes, and T. W. Kenny, J. Appl. Phys. **94**, 4690 (2003).
[15] K. L. Jensen, J. Vac. Sci. Technol. B **21**, 1528 (2003); E. L.

Murphy and R. H. Good, Jr., Phys. Rev. **102**, 1464 (1956); E. Merzbacher, *Quantum Mechanics* (Wiley, New York, 1970); M. Burdick and H.-J. Schmidt, J. Phys. A **27**, 579 (1994).

[16] E. Merzbacher, *Quantum Mechanics* (Wiley, New York, 1970); J. N. Schulman and Y.-C. Chang, Phys. Rev. B **27**, 2346 (1983); S. A. Rakityansky, *ibid.* **70**, 205323 (2004).

[17] W. W. Liu and M. Fukuma, J. Appl. Phys. **60**, 1555 (1986); K. L. Jensen and A. K. Ganguly, *ibid.* **73**, 4409 (1993).

[18] S. Datta, *Electronic Transport in Mesoscopic Systems* (Cambridge University Press, Cambridge, England, 1995); S. Datta, Superlattices Microstruct. **28**, 253 (2000).

[19] D. Mamaluy, D. Vasileska, M. Sabathil, T. Zibold, and P. Vogl, Phys. Rev. B **71**, 245321 (2005).

[20] K. L. Jensen and A. K. Ganguly, J. Appl. Phys. **73**, 4409 (1993); K. L. Jensen, J. Vac. Sci. Technol. B **21**, 1528 (2003).

[21] R. H. Good and E. W. Müller, *Handbook of Physics* (Springer-Verlag, Berlin, 1959), Vol. 21, p. 176.

[22] J. G. Simmons, J. Appl. Phys. **34**, 1793 (1963); G. N. Hatsopoulos and E. P. Syftopoulos, *Thermionic Energy Conversion Volume I: Processes and Devices* (MIT, London, 1973); M. M. Morse and H. Feshbach, *Methods of Theoretical Physics* (McGraw-Hill, New York, 1953), pp. 814–815.

[23] N. D. Lang and W. Kohn, Phys. Rev. B **7**, 3541 (1973); V. E. Kenner, R. E. Allen, and W. M. Saslow, *ibid.* **8**, 576 (1973); A. Zangwill, *Physics at Surfaces* (Cambridge University Press, Cambridge, 1992), pp. 57–63.

[24] V. Rojansky, *Quantum Mechanics* (Prentice-Hall, Englewood Cliffs, NJ, 1938).

[25] M. S. Chung, P. H. Cutler, N. M. Miskovsky, and T. E. Sullivan, J. Vac. Sci. Technol. B **12**, 727 (1994).

[26] T. S. Fisher and D. G. Walker, ASME J. Heat Transfer **124**, 954 (2002).

[27] M. F. O'Dwyer, R. A. Lewis, and C. Zhang, Phys. Rev. B **72**, 205330 (2005); G. N. Hatsopoulos and E. P. Syftopoulos, *Thermionic Energy Conversion Volume I: Processes and Devices* (MIT, London, 1973).

[28] V. S. Fomenko, *Handbook of Thermionic Properties* (Plenum, New York, 1966).

[29] I. Langmuir and K. H. Kingdon, Proc. R. Soc. London, Ser. A **107**, 61 (1925); A. H. Sommer, *Photoemissive Materials* (Krieger, New York, 1980).

[30] R. H. Huang and J. L. Dye, Chem. Phys. Lett. **166**, 133 (1990); J. L. Dye, Science **301**, 607 (2003).

[31] G. S. Nolas and H. J. Goldsmid, J. Appl. Phys. **85**, 4066 (1999).

[32] J. P. Barbour, W. W. Dolan, J. K. Trolan, E. E. Martin, and W. P. Dyke, Phys. Rev. **92**, 45 (1953).

[33] P. C. W. Davies, Am. J. Phys. **73**, 23 (2005); R. Landauer and T. Martin, Rev. Mod. Phys. **66**, 217 (1994).